Catalysis Today 175 (2011) 12–17

Contents lists available at ScienceDirect

Catalysis Today

journal homepage: www.elsevier.com/locate/cattod

Effect of SO_2 on Co sites for NO-SCR by CH_4 over Co-Beta

Shuwei Chen[a], Xiaoliang Yan[b], Yan Wang[b], Jiaqi Chen[b], Dahai Pan[a], Jinghong Ma[b], Ruifeng Li[a,b,*]

[a] College of Chemistry and Chemical Engineering, Taiyuan University of Technology, Taiyuan 030024, China
[b] Institute of Special Chemicals, Taiyuan University of Technology, Taiyuan 030024, China

ARTICLE INFO

Article history:
Received 15 October 2010
Received in revised form 23 April 2011
Accepted 24 May 2011
Available online 22 June 2011

Keywords:
Sulfur dioxide
Nitrogen oxides
Co-Beta
Selective catalytic reduction

ABSTRACT

The activity and stability of the Co-Beta catalyst were investigated for the selective catalytic reduction (SCR) of NO by CH_4 with and without the presence of SO_2. The Co-Beta catalyst exhibited good stability during a long-term test of 30 h for the SCR reaction in the absence of SO_2. The addition of 78 ppm SO_2 caused a decrease in NO conversion, but the loss of catalytic activity was completely reversible after removal of SO_2 from the feed. The characterization of fresh and used Co-Beta catalyst samples by XRD, UV–vis spectroscopy, H_2-TPR, NO-TPD and FTIR spectroscopy was carried out to study the effect of SO_2 on Co sites. UV–vis spectroscopy and H_2-TPR analyses showed that the main Co species present in the catalyst were negligibly reducible Co^{2+} ions located at ion exchange sites and easily reducible polynuclear and/or nanosized Co oxide phases. The poisoning effects of SO_2 on the different Co species were different. The poisoning of SO_2 was irreversible for the Co^{2+} ions at the exchange sites but was completely reversible for the polynuclear and/or nanosized Co oxide species. The reversible deactivation was strongly related to the redox properties of the surface Co species. The polynuclear and/or nanosized Co oxide species were found to be active sites in the SCR reaction.

1. Introduction

The emission of nitrogen oxides (NO_x) from stationary and mobile sources causes serious environmental problems, such as acid rain and photochemical smog. The selective catalytic reduction (SCR) of NO_x with hydrocarbons in an excess of oxygen appears to be a promising method to eliminate NO_x from flue exhaust gases [1–7]. Among various hydrocarbons, methane has received great attention due to its widespread availability and easy handing [8–32]. Zeolite-supported catalysts are the most notable catalysts for CH_4-SCR. It has been shown that Co^{2+} ion-exchange zeolites, such as Co–ZSM-5 [1,8–11], Co–ferrierite [12–14], Co-Beta [15,16], Co–mordenite [17,18] and Co-Beta/Y [19], exhibit high activity in the CH_4-SCR of NO_x. In addition to Co^{2+}, other metal ions, such as Mn^{2+}, Ag^{+}, In^{3+} and Pd^{2+}, can also catalyze the CH_4-SCR reaction [20–26]. However, exhaust gases usually contain water vapor and sulfur dioxide, which may cause extensive deactivation of the catalyst. Therefore, the tolerances of the catalysts are essential for the successful commercial application of the catalytic process. The influence of H_2O on catalytic performance has been extensively studied for several catalysts to date. However, the effect of SO_2 on the rate of NO reduction is not sufficiently covered in the current literature for revealing the cause of the catalyst deactivation by SO_2.

The effect of SO_2 with and without H_2O in the feed gas stream on the deNO_x efficiency of the Co/ZSM-5 and Co/ferrierite catalysts for the reduction of NO by CH_4 was reported by Li and Armor [33]. The effect of SO_2 on the catalytic performance for the reduction without H_2O strongly depends on the type of catalyst and on the reaction temperature, primarily due to the poisoning of the cobalt ionic sites on the catalyst surface by sulfur. Chupin et al. [34] reported that the activity of Co–ZSM-5 for NO reduction by CH_4 was reduced by the presence of SO_2 and only partially recovered after removal of SO_2. Li et al. [28] observed a slight decrease in the NO conversion over Co/SZ in the presence of SO_2, while the Co/SZ returned to its original conversion efficiency after removal of SO_2 from the feed. However, they did not characterize the catalyst deactivated by SO_2 to determine the cause of the catalyst deactivation by SO_2. Recently, She et al. [35] also reported a stabilization effect on the structure and activity of Ag/Al_2O_3 for the SCR of NO_x with CH_4 in the presence of SO_2. The catalyst performance was reversible over many cycles of operation with the SO_2 switched on and off in the gas mixture. They suggested that the presence of SO_2 kept the silver species in a dispersed state on alumina and suppressed deactivation.

The Co-Beta catalyst has high activity, selectivity and resistance to water for NO reduction by CH_4 [15]. However, the influence of SO_2 on the performance and structure of the Co-Beta catalyst is

* Corresponding author at: Taiyuan University of Technology, College of Chemistry and Chemical Engineering, Taiyuan 030024, China. Tel.: +86 351 6010121; fax: +86 351 6010121.
E-mail addresses: ruifeng_li@hotmail.com, rfli@tyut.edu.cn (R. Li).

0920-5861/$ – see front matter © 2011 Elsevier B.V. All rights reserved.
doi:10.1016/j.cattod.2011.05.024

still unclear. The objective of this work was to obtain some useful information on the tolerance of the Co-Beta catalyst to SO_2 by investigating the effect of SO_2 on Co sites. To this end, catalytic tests and deactivation studies were performed together with a thorough characterization of fresh and used catalysts in different conditions by means of XRD, UV–vis spectroscopy, H_2-TPR, NO-TPD and FT-IR spectroscopy.

2. Experimental

2.1. Catalyst preparation

Na-Beta zeolite was synthesized with silica sol ($[SiO_2]$ = 6.02 mol/l), $NaAlO_2$, $NH_3{\cdot}H_2O$, NaOH, and tetraethylammonium bromide [36]. In a typical reaction, 14.50 g of tetraethylammonium bromide (96 wt.%), 14.5 ml of ammonia water (27 wt.%), 1.73 g of sodium aluminate (41 wt.% Al_2O_3, 35 wt.% Na_2O) and 0.94 g of sodium hydroxide (96 wt.%) were dissolved in 25 ml of water to form a clear solution, and 42 ml of silica sol (29 wt.%) was then slowly added to the solution under stirring. The gel was stirred for 2 h at room temperature and then transferred into a 100 ml autoclave and crystallized at 140 °C for 192 h. The product was filtered, washed, and dried at 120 °C for 8 h. Some samples were further calcined at 600 °C for 6 h in an air flow with a heating rate of 1 °C/min. The calcined Na-zeolites sample was ion-exchanged three times with 0.5 M NH_4NO_3 aqueous solution at room temperature. Then, the solid fraction was thoroughly washed, dried at 110 °C overnight, and calcined at 600 °C for 3 h to obtain H-zeolite samples, which were subsequently ion-exchanged using 0.01 M $Co(CH_3COO)_2$ solution at 80 °C for 24 h. The obtained solid sample was washed with distilled water, dried at 120 °C for 6 h, and then calcined at 600 °C for 4 h. The cobalt content of the Co-Beta catalyst was 2.3 wt.% (SiO_2/Al_2O_3 = 35).

2.2. Catalytic test

The catalytic reaction was performed in a quartz tube reactor with a diameter of 6.0 mm in which approximately 300 mg of catalyst was loaded. The catalyst was heated under He flow from room temperature to the reaction temperature, and a mixture of 2180 ppm NO–2050 ppm CH_4–2% O_2 (He balance) was then fed over the catalyst. The total flow rate was 75 ml/min (i.e., GHSV = 7500 h^{-1}). The effluent gas was analyzed by a TCD gas chromatograph (Shimadzu GC-9A) with a packed zeolite 5A column for N_2, CO, O_2, and CH_4 and a packed Porapak Q column for N_2O and CO_2. The NO conversion was calculated from the yield of N_2, and the methane conversion was calculated from its consumption, as described in our previous work [19].

A reactor with two inlets was used to minimize the contamination of the system by SO_2 exposure. The SO_2/He mixture was added to the reactor by a separate inlet. The concentration of SO_2 in the feed was 78 ppm.

2.3. Catalyst characterization

The XRD patterns were recorded using a Rigaku D/max X-ray diffractometer, which employed Ni-filtered Cu Kα radiation and was operated at 40 kV and 80 mA. The powder diffractograms of the samples were recorded over a range of 2θ values from 5 to 40° at a scanning rate of 5° min^{-1}.

DR UV–vis spectra were recorded using a Cary 300 apparatus in the range 200–800 nm. The data were collected and analyzed at the rate of 600 nm/min by a computer.

H_2-TPR experiments were carried out using a SORPTMATIC 1990 instrument. The catalysts were pretreated in air for 30 min at 550 °C. After cooling to room temperature, 10% H_2/Ar (50 ml/min) was introduced in the system, and the temperature was increased to 900 °C at a heating rate of 10 °C/min. The consumption of H_2 was analyzed with a thermal conductivity detector (TCD).

The BET surface area of the catalysts was measured at −196 °C on a NOVA 1200e apparatus by using N_2 adsorption/desorption isotherms.

NO-TPD was carried out using a fixed-bed micro-reactor system. A catalyst charge of 200 mg was used. A sample was pretreated at 500 °C in 50 ml/min He flow for 1 h. Alternatively, the catalyst was allowed to undergo a steady-state NO/CH_4/O_2 reaction in the presence of SO_2 at 600 °C for 2 h and was then flushed with He at the same temperature for 1 h. In both cases, the temperature was decreased to room temperature in flowing He. The NO adsorption was carried out at room temperature by a gas stream of 2000 ppm NO in He at 50 ml/min to achieve saturated adsorption. Then, the catalysts were purged with He at 100 ml/min for 1 h to remove gas-phase NO and weakly adsorbed NO. The TPD run was started from room temperature to 500 °C at a ramping rate of 10 °C/min. The effluent gases from the reactor were continuously monitored using a hand-held combustion analyzer (Kane 940, UK).

FTIR spectra using NO as a probe molecule were recorded on a Shimadzu FTIR-Affinity-1 spectrometer (resolution 4 cm^{-1}). Finely ground samples were pressed in self-supporting thin wafers and then placed in situ in an IR cell equipped with a CaF_2 window. The activation step was performed at a temperature of 400 °C for 2 h in a high vacuum system. Spectra of the activated samples were used as a background reference. NO was introduced into a cell in which the wafer was maintained at RT for 20 min. All the spectra presented were obtained by subtraction of the corresponding background reference.

3. Results

3.1. Catalytic performance of Co-Beta

Fig. 1 shows the changes in the NO and CH_4 conversions with reaction temperature on Co-Beta in the absence of SO_2. The NO conversion rate first increased with reaction temperature, reaching a maximum rate at 600 °C, and the NO conversion then decreased with a further increase in reaction temperature. The CH_4 conversion increased monotonically with reaction temperature over the entire investigated range. As has been reported frequently in the literature, CH_4 is consumed via two parallel reactions, the reduction

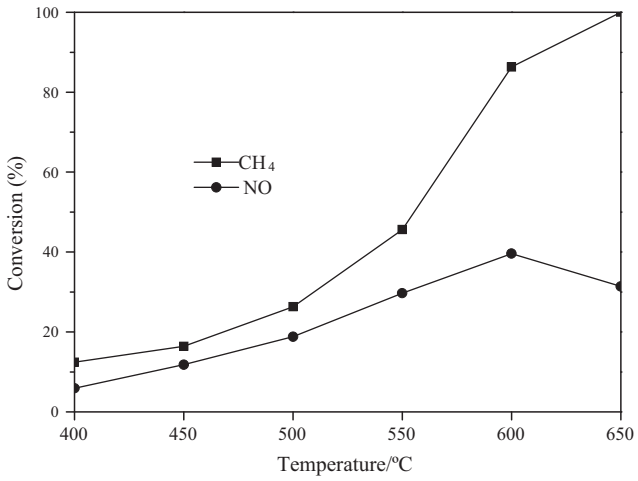

Fig. 1. NO and CH_4 conversion on the Co-Beta catalyst. Reaction conditions: 2180 ppm NO, 2050 ppm CH_4, 2% O_2 and He as the balance; GHSV = 7500 h^{-1}.

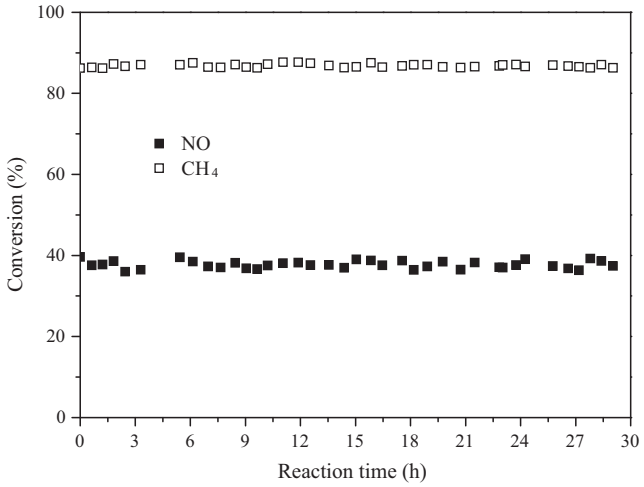

Fig. 2. Catalytic stability of the Co-Beta catalyst at 600 °C. Reaction conditions: 2180 ppm NO, 2050 ppm CH_4, 2% O_2, and He as the balance; GHSV = 7500 h^{-1}.

of NO_x and the combustion by O_2. At higher reaction temperatures (above 600 °C), the combustion of CH_4 dominates over the reaction with NO. Less methane is available for SCR, and the conversion of NO drops. The stability of Co-Beta in the absence of SO_2 is also reported here, and as shown in Fig. 2, the conversion of NO and CH_4 remained unchanged over 30 h at 600 °C, which is the optimum temperature for this catalyst, indicating that the Co-Beta catalyst has a good stability.

3.2. Effect of SO_2 on the performance of Co-Beta

The conversion of NO and CH_4 over Co-Beta in the presence of SO_2 is shown in Fig. 3. When 78 ppm SO_2 was added to the feed at 600 °C, the NO conversion quickly increased from 39% to 70%, then gradually decreased with time and reached a stable level of 32% in approximately 3 h, while the CH_4 conversion continuously decreased from 84% to 66% and then stayed constant. The result is very similar to the observations of Li and Armor over Co/ZSM-5 catalyst [33]. The significant initial increase in NO conversion and the decrease in CH_4 conversion are probably related to the preferentially deposition of SO_2 on the active sites for CH_4 combustion

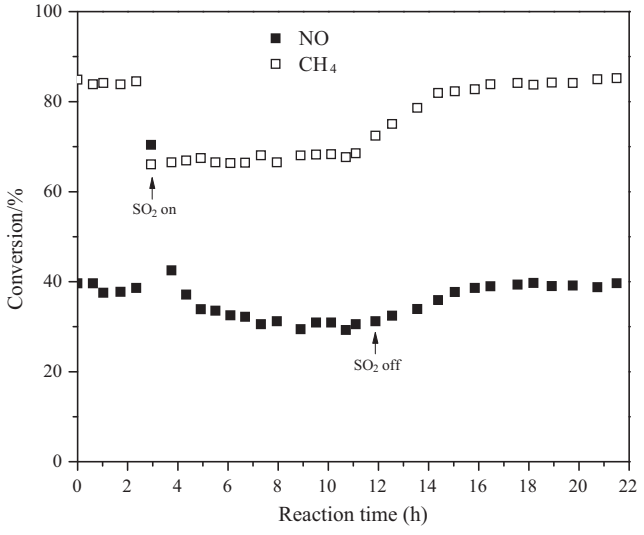

Fig. 3. Effect of SO_2 on the catalytic activities of the Co-Beta catalyst at 600 °C. Reaction conditions: 2180 ppm NO, 2050 ppm CH_4, 2% O_2, 78 ppm SO_2 and He as the balance; GHSV = 7500 h^{-1}.

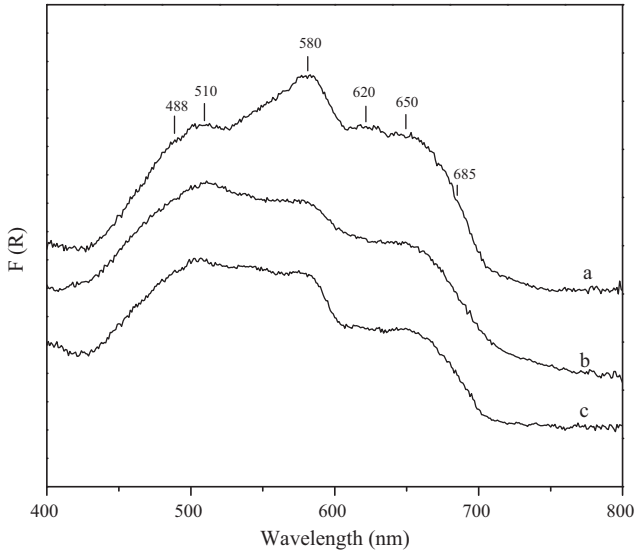

Fig. 4. UV–vis spectra of fresh and used Co-Beta catalysts: (a) fresh catalyst; (b) used catalyst after reaction with SO_2; (c) used catalyst after removal of SO_2.

[33,34], which greatly enhances the selectivity of CH_4 toward NO reduction as the result of SO_2 addition. Obviously, the first portion of SO_2 deposited on the catalyst has the highest impact on the conversion of NO and CH_4, and the steady-state conversion rate obtained after 3 h in the presence of SO_2 indicated an achievement of an equilibrium condition for adsorption and desorption of SO_2 [33]. After removal of SO_2 from the feed, the conversion of NO and CH_4 returned to its original level, suggesting that the poisoning effect of SO_2 is completely reversible for Co-Beta.

3.3. Detection of cobalt species

The XRD pattern of the used Co-Beta catalyst after reaction for 10 h with 78 ppm SO_2 at 600 °C presents the typical pattern of a BEA zeolite and is almost unchanged relative to the spectrum of fresh Co-Beta (not shown). This result indicated that introducing SO_2 into the feed did not affect the crystal structure of the catalyst. The absence of reflexes corresponding to crystalline oxide phases of CoO or Co_3O_4 confirm that Co is present either in the exchanged position of the zeolite or in the shape of Co aggregates <3 nm in size.

Fig. 4 shows the UV–vis spectra of fresh Co-Beta catalyst and used catalysts before and after removal of SO_2 from the feed. Adsorption bands at approximately 685, 650, 620, 580, 510, and 488 nm were observed for fresh Co-Beta catalyst. No other absorption occurred in the range 200–400 nm. The spectra that we observed were similar to those reported and discussed in detail by Dedecek et al. for Co-Beta and other Co–H zeolites [37,38]. The band at 685 nm could be ascribed to α-type Co^{2+} ions (formed above an elongated 6-MR composed of twofold-connected 5-MR in the polymorph C). The quartet bands at 650, 620, 580, and 488 nm could be attributed to β-type Co^{2+} ions (located at the position close to the plane of the deformed six-membered ring (MR) of the hexagonal cage present in polymorphs A and B), and the band at 510 nm is characteristic of γ-type Co^{2+} ions (inside the hexagonal cage of polymorphs A and B). The UV–vis spectra of the used catalyst after reaction for 10 h with 78 ppm SO_2 show that the bands belonging to β-type Co^{2+} ions strongly decreased in intensity, and the intensity of these bands was almost unchanged for the used catalyst after removal of SO_2 from the feed, suggesting that the adsorption of SO_2 led to an irreversible change in the Co ions located in the β-position.

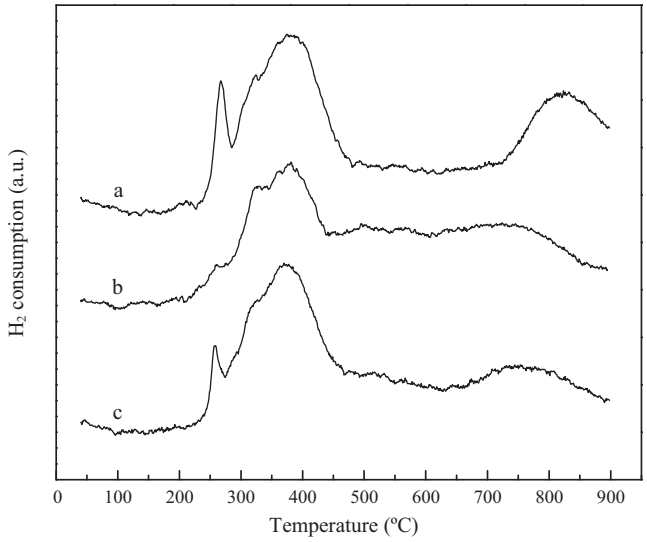

Fig. 5. H_2-TPR curves of fresh and used Co-Beta catalysts: (a) fresh catalyst; (b) used catalyst after reaction with SO_2; (c) used catalyst after removal of SO_2.

Fig. 5 shows the results of the H_2-TPR measurements obtained for fresh and used Co-Beta under different conditions. The spectrum of fresh Co-Beta showed three peaks at 260, 375, and 820 °C. The reduction peak at 820 °C could be attributed to Co^{2+} in the exchange sites [11,39,42], which should be more resistant to reduction because it is stabilized by the negatively charged zeolite framework. The TPR peaks appearing at lower temperatures were attributed to an easily reducible cobalt oxide phase, possibly made up of polynuclear Co oxo-ions and/or nanosized particles that are not detectable by the above characterization techniques (XRD, UV–vis) [40]. After reaction for 10 h with 78 ppm SO_2, the Co-Beta catalyst showed a markedly different TPR profile (Fig. 5(b)) in which the peaks of all Co species strongly decreased, and the reduction peak for Co ions at exchange sites shifted to a lower temperature, probably due to the location of these ions in more accessible positions. Moreover, a new peak in the 450–600 °C region was observed, corresponding to the reduction of CoO_x located inside the zeolite channels [42]. After removal of SO_2 from the feed, the intensity of the TPR peaks at higher temperatures, corresponding to Co^{2+} in the exchange sites, did not change significantly, while the intensity of peaks at lower temperatures, corresponding to polynuclear and/or nanosized Co oxide phases, returned to their original levels. This tendency is in good agreement with the NO reduction activity.

3.4. BET surface area and NO-TPD characterization

The surface area of the catalyst after reaction for 10 h with 78 ppm SO_2 at 600 °C decreased from 360 m^2/g for the fresh catalyst to 316 m^2/g. A surface area loss of approximately 12% for the Co-Beta catalyst was observed when it was exposed to SO_2. However, the surface area of the used catalyst after removal of SO_2 from the feed (340 m^2/g) was similar to that of the fresh catalyst.

The effect of SO_2 on the adsorption of NO was examined by measuring the NO uptake capacity of the fresh and used catalysts under different conditions. As shown in Fig. 6, two NO desorption peaks were observed at approximately 160 °C and 300 °C in the NO-TPD profile of the fresh catalyst. The intensity of the desorption peaks was lower for the used catalyst both before and after removal of SO_2 from the feed. However, the desorption peaks of the catalyst after reaction for 10 h with 78 ppm SO_2 at 600 °C were smaller than those after the removal of SO_2 from the feed. The result agrees well with the BET surface area trends. These results clearly suggest that adding SO_2 induces the loss of Co sites, therefore resulting in a decrease in the SCR activity [33,43], and that removing SO_2 from the feed leads to partial recovery of Co sites, probably due to the irreversible poisoning of Co^{2+} ions at exchange sites. The introduction of SO_2, however, did not influence the SCR activity of the catalyst after removal of SO_2 from the feed [44].

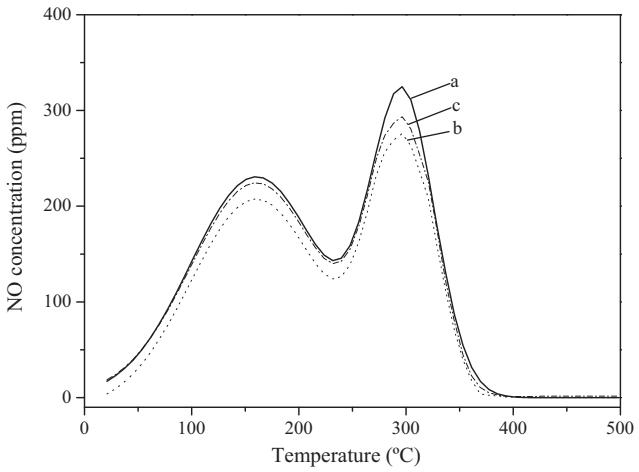

Fig. 6. NO-TPD profiles of the fresh and used Co-Beta catalysts: (a) fresh catalyst; (b) used catalyst after reaction with SO_2; (c) used catalyst after removal of SO_2.

3.5. FTIR information of NO_y species

NO_y species formed on the catalyst surface are known to play an important role in the SCR of NO by CH_4 [9,18,39,40]. The influence of SO_2 on the FTIR spectra of surface species was examined. Infrared spectra of surface species formed from NO over the fresh and used Co-Beta after reaction for 10 h with 78 ppm SO_2 are shown in Fig. 7. Five bands were observed at 1934, 1897, 1841, 1630, and 1530 cm^{-1}. The doublet at 1814 cm^{-1} and 1897 cm^{-1} was assigned to Co^{2+}–dinitrosyl species, and the band at 1530 cm^{-1} was attributed to NO_3^- species [9,18]. The band at 1934 cm^{-1} suggests the presence of Co^{3+}–mononitrosyls [ix], while the band at 1630 cm^{-1} is due to adsorbed water [9,18]. After reaction for 10 h with 78 ppm SO_2, the bands for the Co^{2+}–-dinitrosyl species, Co^{3+}–mononitrosyls and NO_3^- species decreased in intensity, while the band for adsorbed water significantly increased in intensity, which may be due to the competition between water and NO species for the chance to adsorb to the active sites. These results

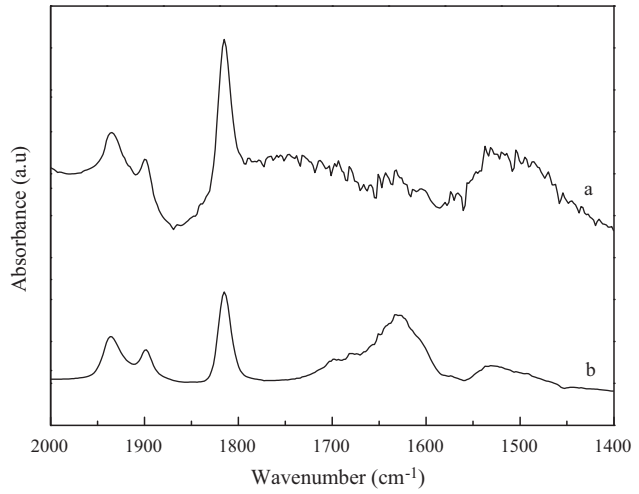

Fig. 7. FT-IR spectra of surface species arising from the adsorption of NO on Co-Beta catalysts: (a) fresh catalyst; (b) used catalyst after reaction with SO_2.

indicate that the addition of SO_2 to the feed inhibits the adsorption of NO species and promotes the adsorption of water on the active sites.

4. Discussions

Different hypotheses have been reported in recent literature on the nature of the active sites that participate in the NO-SCR reaction. Co^{2+} ions exchanged in the zeolitic matrix [11,45], Co^{3+} and multinuclear Co-oxide particles [17,41,42] and cobalt–oxygen microaggregates [34] have been suggested to be involved in the SCR of NO with CH_4. The reduction of NO by CH_4 in the presence of O_2 involves two molecules of NO, one molecule of CH_4, and one molecule of O_2 ($CH_4 + 2NO + O_2 \rightarrow N_2 + CO_2 + 2H_2O$), and at least several elementary steps are generally accepted [40]. The reaction mechanism inferred that the reaction of all of these molecules on isolated sites is highly unlikely [34]. TPR data obtained in the present work showed that Co^{2+} ions exchanged in Beta zeolites were reduced by hydrogen at approximately 800 °C; therefore, it is unlikely that such species could be reduced under the reaction conditions. Moreover, the number of Co^{2+} sites at ion exchange sites did not significantly change before and after removal of SO_2 from the feed (Figs. 4 and 5). However, our experimental data indicate that the poisoning effect of SO_2 was completely reversible for Co-Beta (Fig. 3). Therefore, isolated Co^{2+} ions at exchange sites cannot be considered active sites. On the other hand, far more easily reducible species were detected from TPR low-temperature signals. Moreover, the intensity of peaks at lower temperatures, corresponding to polynuclear and/or nanosized Co oxide phases, almost returned to their original levels after removal of SO_2 from the feed (Fig. 5), which is in good agreement with the tendency of the catalytic activity of Co-Beta. Therefore, these results suggest that polynuclear and/or nanosized Co oxide species are active sites for the SCR of NO by CH_4 on Co-Beta.

Two parallel reactions, i.e., NO reduction by CH_4 and CH_4 combustion by O_2, occur simultaneously during the reaction. The decline in CH_4 conversion combined with a significant increase in NO conversion meant that the selectivity of the reaction for NO reduction was enhanced by the addition of SO_2 during the initial period. This result suggests that SO_2 preferentially adsorbed to Co oxides presents on the zeolite's outer surface that were less selective for NO reduction but more active for CH_4 combustion [33,34]. With increased reaction time, SO_2 gradually adsorbed onto other Co sites until an equilibrium condition for the adsorption and desorption of SO_2 was achieved. As shown in Fig. 6, the decrease in the capacity for NO adsorption demonstrated that some Co sites were occupied due to SO_2 exposure, which resulted in a decrease in the number of active sites and in the amount of the adsorbed NO_3^- intermediate. As a result, the catalytic activity decreased. Removing SO_2 from the feed led to a recovery of the multinuclear Co active sites, therefore resulting in a higher NO uptake and the reversible loss of SCR activity.

It is worth noting that the poisoning by SO_2 was irreversible for the Co^{2+} ions at exchange sites but was completely reversible for the polynuclear and/or nanosized Co oxide species. These results support the hypothesis that the effect of SO_2 on different Co species was different in poisoning mechanism. As shown in Fig. 5, the reduction peak of Co ions at exchange sites shifted to a lower reduction temperature, and its intensity decreased due to the formation of CoO_x species in the presence of SO_2. Moreover, the intensity of the Co ion reduction peak was unchanged after removal of SO_2 from the feed, which was consistent with the UV–vis DRS results (Fig. 4). These results suggested that the conversion of cobalt from isolated Co ions (probably in β-sites) into CoO_x species occurred and was irreversible. As shown in Fig. 7, the adsorption of H_2O was promoted in the presence of SO_2, which could speed up this conversion process by hydrating the cations and further agglomerating to form the (Co–O) species [34,42,46]. The reversible poisoning of the polynuclear and/or nanosized Co oxide species by SO_2 was probably related to their redox properties. The reaction of SO_2 might take place on the surface of the polynuclear and/or nanosized Co oxide species: $3SO_{2(a)} \rightarrow 2SO_{3(a)} + S_{(a)}$. SO_3 was thermally desorbed, and the atomic sulfur reacted with the surface oxygen on the polynuclear and/or nanosized Co oxide species: $S_{(a)} + 2O_{(a)} \rightarrow 2SO_{2(g)}$. The polynuclear and/or nanosized Co oxide species were therefore reduced [47]. Then, the reduced Co oxides were oxidized by O_2 and returned to their original oxidation state after removal of SO_2 from the feed.

5. Conclusions

It was demonstrated that the Co-Beta catalyst exhibits good stability in the SCR of NO with methane. The addition of SO_2 decreased the catalyst activity of Co-Beta. After removal of SO_2 from the feed, Co-Beta returned to its original conversion level. Co^{2+} ions at exchange sites and polynuclear and/or nanosized Co oxide phases coexist in the Co-Beta catalyst. The easily reducible polynuclear and/or nanosized Co oxide species were found to be the active sites for the SCR reaction. The poisoning by SO_2 of different Co species occurs by different poisoning mechanisms. SO_2 induced the irreversible conversion of cobalt from isolated Co ions (probably in β-sites) into CoO_x species. However, the poisoning by SO_2 of the polynuclear and/or nanosized Co oxide species was completely reversible, probably due to the high redox properties of these Co oxide species. This reversible deactivation could be attributable to the facile redox transformation of polynuclear and/or nanosized Co oxide species.

Acknowledgments

This work was supported by the Natural Science Foundation of China (20876102), the Research Fund for the Doctoral Program of Higher Education (200801120006), and the Natural Science Foundation of Shanxi Province of China (2008011022).

References

[1] Y. Li, J.N. Armor, Appl. Catal. B 1 (1992) L31.
[2] J.N. Armor, Catal. Today 26 (1995) 147.
[3] M. Shelef, Chem. Rev. 95 (1995) 209.
[4] Y.H. Chin, W.E. Alvarez, D.E. Resasco, Catal. Today 62 (2000) 159.
[5] V. Indovina, D. Pietrogiacomi, M.C. Campa, Appl. Catal. B 39 (2002) 115.
[6] A. Wang, D. Liang, C. Xu, X. Sun, T. Zhang, Appl. Catal. B 32 (2001) 205.
[7] X.Y. Chen, S.C. Shen, H.H. Chen, S. Kawi, J. Catal. 221 (2004) 137.
[8] L.J. Lobree, A.W. Aylor, J.A. Reimer, A.T. Bell, J. Catal. 169 (1997) 188.
[9] T. Montanari, O. Marie, M. Daturi, G. Busca, Appl. Catal. B 71 (2007) 216.
[10] J. Zhang, Y. Liu, W. Fan, Y. He, R. Li, Fuel 86 (2007) 1577.
[11] P.J. Smeets, Q. Meng, S. Corthals, H. Leeman, R.A. Schoonheydt, Appl. Catal. B 84 (2008) 505.
[12] T.J. Lee, I.S. Nam, S.W. Ham, Y.S. Baek, K.H. Shin, Appl. Catal. B 41 (2003) 115.
[13] J.H. Park, C.H. Park, I.S. Nam, Appl. Catal. A 277 (2004) 271.
[14] S. Capela, R. Catalao, M.F. Ribeiro, P.D. Costa, G.D. Mariadassou, F.R. Ribeiro, C. Henriques, Catal. Today 137 (2008) 157.
[15] H.H. Chen, S.C. Shen, X. Chen, S. Kawi, Appl. Catal. B 50 (2004) 37.
[16] A.P. Ferreira, C. Henriques, M.F. Ribeiro, F.R. Ribeiro, Catal. Today 107–108 (2005) 181.
[17] T. Montanari, O. Marie, M. Daturi, G. Busca, Catal. Today 110 (2005) 339.
[18] F. Lonyi, J. Valyon, L. Gutierrez, M.A. Ulla, E.A. Lombardo, Appl. Catal. B 73 (2007) 1.
[19] J. Zhang, W. Fan, Y. Liu, R. Li, Appl. Catal. B 76 (2007) 174.
[20] M.C. Campa, D. Pietrogiacomi, S. Tuti, G. Ferraris, V. Indovina, Appl. Catal. B 18 (1998) 151.
[21] Q. Sun, W.M.H. Sachtler, Appl. Catal. B 42 (2003) 393.
[22] Z. Li, M. Flytzani-Stephanopoulos, J. Catal. 182 (1999) 313.
[23] C. Shi, M. Cheng, Z. Qu, X. Bao, J. Mol. Catal. A 235 (2005) 35.
[24] L. Ren, T. Zhang, J. Tang, J. Zhao, N. Li, L. Lin, Appl. Catal. B 41 (2003) 129.
[25] T. Maunula, J. Ahola, H. Hamada, Appl. Catal. B 64 (2006) 13.
[26] L.J. Lobree, A.W. Aylor, J.A. Reimer, A.T. Bell, J. Catal. 181 (1999) 189.

[27] C.N. Costa, T. Anastasiadou, A.M. Efstathiou, J. Catal. 194 (2000) 250.
[28] N. Li, A.Q. Wang, J.W. Tang, X.D. Wang, D.B. Liang, T. Zhang, Appl. Catal. B 43 (2003) 195.
[29] N. Li, A. Wang, Z. Liu, X. Wang, M. Zheng, Y. Huang, T. Zhang, Appl. Catal. B 62 (2006) 292.
[30] X. She, M. Flytzani-Stephanopoulos, J. Catal. 237 (2006) 79.
[31] G.H. Jing, J.H. Li, D. Yang, J.M. Hao, Appl. Catal. B 91 (2009) 123.
[32] G.H. Jing, J.H. Li, D. Yang, J.M. Hao, Chin. J. Catal. 30 (2009) 459.
[33] Y. Li, J.N. Armor, Appl. Catal. B 5 (1995) L257.
[34] C. Chupin, A.C. van Veen, M. Konduru, J. Despres, C. Mirodatos, J. Catal. 241 (2006) 103.
[35] X. She, M. Flytzani-Stephanopoulos, C. Wang, Y. Wang, C.H.F. Peden, Appl. Catal. B 88 (2009) 98.
[36] J.J. Zheng, J.H. Ma, Y. Wang, Y.D. Bai, X.W. Zhang, R.F. Li, Catal. Lett. 130 (2009) 672.
[37] J. Dedecek, L. Capek, D. Kaucky, Z. Sobalik, B. Wichterlova, J. Catal. 211 (2002) 198.
[38] J. Dedecek, B. Wichterlova, J. Phys. Chem. B 103 (1999) 1462.
[39] X. Wang, H. Chen, W.M.H. Sachtler, Appl. Catal. B 29 (2001) 47.
[40] C. Resini, T. Montanari, L. Nappi, G. Bagnasco, M. Turco, G. Busca, F. Bregani, M. Notaro, G. Rocchini, J. Catal. 214 (2003) 179.
[41] G. Bagnasco, M. Turco, C. Resini, T. Montanari, M. Bevilacqua, G. Busca, J. Catal. 225 (2004) 536.
[42] A. Martinez-Hernandez, G.A. Fuentes, Appl. Catal. B 57 (2005) 167.
[43] M.H. Kim, I.S. Nam, Y.G. Kim, J. Catal. 179 (1998) 350.
[44] Z. Li, M.F. Stephanopoulos, Appl. Catal. B 22 (1999) 35.
[45] D. Kauchy, A. Vondrova, J. Dedechek, B. Wichterlova, J. Catal. 194 (2000) 318.
[46] S. Ordonez, J.R. Paredes, F.V. Diez, Appl. Catal. A 341 (2008) 174.
[47] M. Haneda, Pusparatu, Y. Kintaichi, I. Nakamura, M. Sasaki, T. Fujitani, H. Hamada, J. Catal. 229 (2005) 197.